Original Article

FABRICATION AND DEVELOPMENT OF DISSOLVING MICRONEEDLE PATCH OF BUTORPHANOL TARTRATE

AMAN TIWARI [iD], SHUBHAM SHARMA [iD], PRAKASH KUMAR SONI [iD], SURESH KUMAR PASWAN* [iD]

Industrial Pharmacy Research Lab, Department of Pharmacy, Shri G. S. Institute of Technology and Science, 23, Park Road Indore 452003 (M. P), India
Email: skpaswan@gmail.com

ABSTRACT

Objective: Butorphanol is a commonly used medication for the management of postoperative pain and suffers low bioavailability and high first-pass metabolism. The objective of the current studies was to develop a butorphanol tartrate-loaded dissolving microneedle patch to overcome the limitation of first-pass metabolism without causing any discomfort to the patient.

Methods: Butorphanol tartrate-loaded microneedle patch was prepared using Lapox resin micro-molds. The microneedle patch was optimized using the box-Behnken design and the quantity of PVA, HPMC K4M, and HPMC K15M was optimized and evaluated for fractured axial force, microscopic evaluation, *in vitro* drug permeation studies, and *ex-vivo* permeation experiments.

Results: The developed microneedle patch meets all the evaluation parameters within the desired range. The height and tip diameter of the microneedles were found to be 700 μm to 800 μm and 60 μm to 61 μm. An axial fractured force of the optimized microneedle patch was found to be 189.67 N, suitable for penetrating the stratum corneum. The *in vitro* cumulative % drug permeated showed the permeation of the drug for 8 h with a total of 89.12 %, which shows the permeation of the drug occurred in a controlled manner.

Conclusion: Butorphanol tartrate-loaded microneedle patch was successfully developed and the results concluded that the microneedles were hard enough to pass the stratum corneum and release the drug into the systemic circulation without reaching the pain receptors; further, the release study suggested that the drug was released for a prolonged period eliminating the problem of first-pass effect and frequent administration.

Keywords: Butorphanol tartrate, Dissolving microneedles, Lapox resin mould, Mould casting, Axial fractured force, Box-behnken design, Postoperative pain

INTRODUCTION

Postoperative pain results from tissue damage caused after surgical procedures [1]. Inadequate pain management can lead to slower recovery, prolonged hospitalization, and even death. Analgesic medications are commonly required by patients undergoing surgical procedures to effectively manage intense pain [2, 3]. Opioids are commonly administered for severe acute pain management since they provide effective analgesia while preserving sensory and motor function. Opioid medications can effectively manage pain and minimize side effects through the understanding of the mechanism of action and potential adverse effects of the various options available [4]. Morphine, butorphanol, fentanyl, and meperidine are considered standard for treating moderate to severe postoperative pain [5].

Butorphanol tartrate is a mixed agonist-antagonist opioid compound that possesses potent analgesic characteristics. Studies have demonstrated that butorphanol has a higher analgesic potency than morphine, pentazocine, and meperidine, with approximate ratios of 5:1, 20:1, and 40:1, respectively [6]. Conventional formulations for postoperative pain management, including oral, parenteral, and nasal, have drawbacks such as invasiveness, nasal irritation, stomach degradation, and low bioavailability. The oral bioavailability of butorphanol is only 5-17 % due to significant first-pass metabolism. The primary drawbacks of the oral and parenteral routes are eliminated using transdermal drug delivery [7]. The transdermal delivery is a solution for bypassing first-pass metabolism in quickly metabolized drugs. To enhance the permeation of the drug through the skin in transdermal delivery, various methods, such as skin penetration augmentation techniques, have been developed to increase its bioavailability. These mechanisms are highly effective for targeting the delivery of therapeutic agents to the desired site of action. Traditional transdermal delivery systems, such as lotions or patches, are limited to passive permeation of the stratum corneum [8]. This barrier effectively prevents or reduces the transport of most water-soluble medicines.

Transdermal dissolving microneedle patches have been shown to effectively penetrate the stratum corneum and reach the epidermis, thereby increasing the permeability of water-soluble medications to the skin [9-11]. These patches have been designed to minimize pain by avoiding nerve endings in the deeper dermis. Transdermal delivery of butorphanol tartrate is used as an effective pain reliever that offers a safer alternative to the agonist of the μ-opioid receptor.

Microneedles were aimed at providing a cost-effective and dependable method of administering medication to the epidermal layer while minimizing harm to nerve cells and reducing the potential for microbial penetration [12]. Microneedles have various types, including solid microneedles, drug-coated needles, hydrogel-forming needles, and dissolving needles [13-16]. Dissolving microneedles are a type of microneedle technology that utilizes tiny, polymeric needles made of biodegradable and water-soluble polymers containing pharmaceuticals within their matrix [17]. These needles dissolve or break down within the skin, releasing the medication, which can be released for local or systemic distribution over short or extended periods immediately upon insertion into the skin [18-20].

The current study aims to overcome the problem of first-pass metabolism associated with butorphanol tartrate by preparing the dissolving microneedle patch of butorphanol tartrate using the solvent casting method. Box-Behnken design of response surface methodology was used for the formulation and optimization of the butorphanol tartrate-loaded dissolving microneedle patch. The software suggested quantities of independent variables i.e., Polyvinyl alcohol, HPMC K4M, and HPMC K15M, that influences the response variables i.e., axial fractured force and cumulative % drug permeated. To determine the drug permeation, an *ex-vivo* study was also performed. This microneedle array is anticipated to have improved permeability, improved efficacy with fewer side effects, and higher patient compliance when compared to an existing formulation for the treatment of postoperative pain.
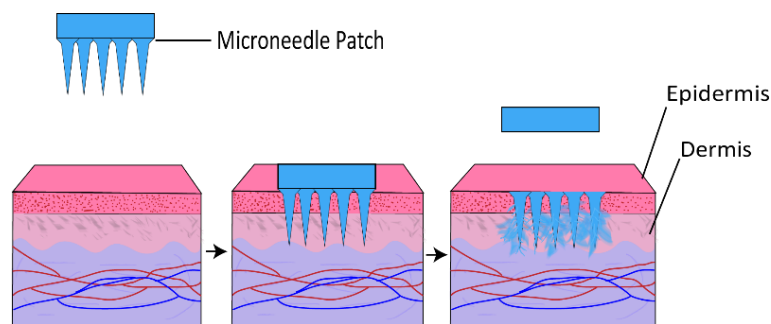
Fig. 1: Schematic diagram of dissolving microneedle patch

MATERIALS AND METHODS

Material

Butorphanol tartrate was procured as a gift sample from Aristo Pharmaceuticals Pvt. Ltd., India. Polyvinyl alcohol (molecular weight, 1,60,000 Da) was purchased from Himedia. HPMC K 4M and HPMC K 15M were received as gift samples from Colorcon. Derma Stamp (L4001, 1.5 mm metal needle length) was bought from online amazon.in and Lapox® hardener was purchased from the local market.

Method

In the current study, the micro-molding/solvent casting method is used to make butorphanol-loaded controlled-release dissolving microneedles for enhanced transdermal delivery. The current process involves two steps. The first step is the preparation of a Lapox® resin micro-mold. The second step is the formulation of a dissolving microneedle patch using a mould casting method. The details of the process are mentioned below [21].

Preparation of epoxy resin micro-mold

Micro moulds were prepared using epoxy resin (Lapox®) and microneedle master structure i.e., (Derma stamp). The derma stamp contains 36 conical microneedles of 1.5 mm in length with a retractable lever. The inverse replica was prepared by mixing the ten parts of the epoxy resin base with one part of the hardening agent. The prepared mixture was transferred into a moulding container, and the container was kept in a vacuum desiccator to remove air bubbles. Further, the derma stamp had been vertically inserted into the solution by pressing the lever and left in place for 24 h for drying. After drying, derma stamp was removed from the container creating microcavities in the prepared micro-mold.

Formulation of dissolving microneedle patch by solvent casting method

A controlled release dissolving microneedle of butorphanol tartrate was fabricated using varying concentrations of polyvinyl alcohol, HPMC K4M, and HPMC K15M. The polymeric solution was prepared using 3 mg of butorphanol tartrate and varying amounts of polymer, as mentioned in table 2, which were dissolved in 10 ml of purified water. 1 ml of a solution containing polymer and drug was transferred into epoxy resin micro moulds and centrifuged at 4500 rpm for 7 min, followed by drying in a vacuum desiccator for 18-24 h. After 24 h, the microneedle patches were pulled from the micro moulds using forceps and carefully preserved in a well-closed container.

Optimization of formulation variables

Experimental design

Optimization with the help of experimental design may help in reduce the experiment time [22]. The optimization studies were carried out of butorphanol tartrate loaded dissolving microneedle patch using Design Expert software. A three-factor, three-level Box-Behnken design was used as an experimental design. According to pre-optimization experiments, the excipient ratio had a significant impact on the properties of microneedles, such as fractured axial force and drug permeation. The factors that influence the desired performance of the final product were considered as independent variables i.e., quantities of PVA, HPMC K4M, and HPMC K15M. The variables that were used to evaluate the performance of the final product were chosen as dependent or response variables i.e., fractured axial force (Y_1), cumulative % drug permeated at 15 min (Y_2), 30 min (Y_3), 60 min (Y_4), 120 min (Y_5), 240 min (Y_6), 360 min (Y_7), and 480 min (Y_8) are shown in table 1.

Table 1: Box-behnken design generated independent variables

Variables	Unit	Lower level	Upper level
A: Polyvinyl alcohol (X_1)	mg	180	220
B: HPMC K4M (X_2)	mg	50	60
C: HPMC K15M (X_3)	mg	20	40
Response variable		Constraint	
Axial fractured force (Y_1)		Maximize	
Cumulative % drug permeated at 15 min (Y_2)		Minimize	
Cumulative % drug permeated at 30 min (Y_3)		Minimize	
Cumulative % drug permeated at 60 min (Y_4)		Minimize	
Cumulative % drug permeated at 120 min (Y_5)		Minimize	
Cumulative % drug permeated at 240 min (Y_6)		Minimize	
Cumulative % drug permeated at 360 min (Y_7)		Minimize	
Cumulative % drug permeated at 480 min (Y_8)		Minimize	

The Box-Behnken design suggested a total of fifteen batches with three centre points based on independent variables, as demonstrated in table 2. The optimization batches of butorphanol tartrate loaded microneedles batches were prepared and evaluated for fractured axial force by using TA-XT plus texture analyser and cumulative % drug permeated by utilizing Franz diffusion cell. The optimization batches of the butorphanol tartrate-loaded microneedle patch were evaluated

for the response variable mentioned, as shown in table 3. The data of response variables of optimization batches were fitted into linear, two factors interaction (2FI), quadratic, and cubic models to assess consistency with, lack of fit, sequential p-values, and predicted and adjusted R-square values, as given in table 4. The 3-D response surface plots are shown in fig. 2 to fig. 17 and the polynomial equation was statistically verified by ANOVA as shown in tables 5.

Table 2: Box-behnken experimental plan for optimization of butorphanol tartrate microneedles batches

S. No.	Batch no.	Quantity of ingredients (mg)		
		PVA	HPMC K4M	HPMC K15M
1	BTMN 1	180	50	30
2	BTMN 2	220	50	30
3	BTMN 3	180	60	30
4	BTMN 4	220	60	30
5	BTMN 5	180	55	20
6	BTMN 6	220	55	20
7	BTMN 7	180	55	40
8	BTMN 8	220	55	40
9	BTMN 9	200	50	20
10	BTMN 10	200	60	20
11	BTMN 11	200	50	40
12	BTMN 12	200	60	40
13	BTMN 13	200	55	30
14	BTMN 14	200	55	30
15	BTMN 15	200	55	30

Evaluation of butorphanol tartrate loaded microneedle patch

Microscopic evaluation

Laser confocal microscopy

Laser confocal microscopy is used to investigate the structure and structural relationships along the optical (z) axis as well as in the x-y plane [23]. The evaluation of the size and shape of the microneedle was done using laser confocal microscopy (Zeiss laser confocal scanning optical microscope. The height, tip diameter, and base diameter of the prepared optimized batch of microneedles (OP-BTMN) were evaluated. The microscopic image of the laser confocal is shown in fig. 21.

Scanning electron microscopy

The surface morphology and size of the microneedle were evaluated by field emission scanning electron microscopy (FE-SEM Supra 55 Zeiss). A patch of butorphanol tartrate-loaded microneedles (OPBTMN) was attached to an aluminum stub with dual-sided carbon tape and exposed to gold fumes and observed under FE-SEM at 2.0 kV. The microscopic image of FE-SEM is shown in fig. 22.

Evaluation of fractured axial force

The axial fracture force refers to the minimum amount of force that needs to be applied along the axis of the microneedle to cause it to deform or break. The behaviour of materials under crushing loads is determined by the hardness of the needle. The fractured axial force of the prepared butorphanol tartrate-loaded microneedles was evaluated using TA-XT plus analyzer. The microneedle patch was mounted to the cylindrical probe using dual-sided adhesive tape and analysed at compression mode. The probe was moved from a 2.5 mm test distance height at the test speed of 0.1 mm/sec with a trigger force of 0.049 N. The sudden fall in the force was considered as the breaking of the needle or needle failure and the maximum force applied just before this drop is recorded as the axial fracture force. The values of the fractured axial force of various optimization batches are shown in table 3 and the optimized batch is shown in table 6. The graph between force (N) and time (sec) of the optimized batch is shown in fig. 23.

Evaluation of drug content

The optimised microneedle patch (OPBTMN) was placed in a beaker with 50 ml of phosphate buffer saline pH 7.4 and stirred for 1 h to dissolve the microneedle patch. The resultant solution was appropriately diluted with phosphate buffer saline pH 7.4 and analysed on UV-spectrophotometer (Shimadzu 1700) at 280 nm. The percentage of drug amount was calculated as per the formula mentioned below.

$$\% \text{ Drug amount} = \frac{(\text{Estimated amount of drug})}{(\text{Total amount drug loaded})}$$

In vitro drug permeation studies

The *in vitro* drug permeation study was conducted on a Franz diffusion cell with a receptor chamber volume of 15 ml. The microneedle patch was inserted into the Parafilm M® and mounted between the donor and receptor chambers. The receptor chamber was filled with phosphate buffer saline pH 7.4 and the solution was stirred with a magnetic stirrer at a temperature of 37 °C±0.5 °C. A 5 ml of sample was withdrawn at the time interval of 15, 30, 60, 120, 240, 360, and 480 min, from the receptor chamber and immediately replaced with fresh phosphate buffer saline pH 7.4. The drug concentration in withdrawn samples was measured using a UV-spectrophotometer (Shimadzu 1700) at 280 nm. The *in vitro* drug permeation data of the optimization batch and optimized batch are shown in table 3 and table 6, respectively and graphically represented in fig. 18 and fig. 24, respectively. The comparison of software-predicted and experimentally observed *in vitro* drug permeation data of the optimized formulation batch is shown in table 6 and fig. 20.

***Ex-vivo* permeation studies**

An *ex-vivo* permeation study of the butorphanol tartrate-loaded microneedle patch was performed to evaluate drug permeation across the biological membrane. The skin of a porcine ear was used in this investigation as a biological membrane due to its resemblance to human skin [24]. In dermatological studies, porcine ear skin is utilized as a substitute for human skin and is helpful for tape-stripping experiments to examine the penetration of active compounds into the topmost skin layers [25]. The ear skin of a 6-month-old porcine was procured from the local market and preserved in saline. The *ex-vivo* permeability of a butorphanol tartrate-loaded microneedle patch was evaluated by the Franz diffusion cell. The receptor chamber was filled with phosphate buffer saline pH 7.4. The whole assembly was placed on a magnetic stirrer and continuously stirred and the temperature was maintained at 37 °C±0.5 °C. A 5 ml of sample was withdrawn at time intervals of 15, 30, 60, 120, 240, 360, and 480 min from the receptor chamber and immediately replaced with fresh phosphate buffer saline pH 7.4. The drug concentration in withdrawn samples was measured using a UV-spectrophotometer (Shimadzu 1700) at 280 nm. The graph was plotted between the cumulative % drug permeated per cm^2 and time, as shown in fig. 25. The steady-state flux (J_{ss}, $g/cm^2/h$) was calculated using the slope of the linear section of the graph between cumulative % drug permeated per cm^2 vs time. The permeation enhancement ratio (PER) from steady-state flow in comparison to plain drug solution (PDS) was calculated using a formula mentioned below,

$$\text{Permeation enhancement ratio} = \frac{J_{ss}^{BTMN}}{J_{ss}^{PDS}}$$

Where, J_{ss}^{BTMN}, the flux at steady state of optimized batcha

J_{ss}^{PDS} is flux at a steady state of plain drug solution.

RESULTS AND DISCUSSION

Optimization of butorphanol tartrate-loaded microneedle

The optimization of the butorphanol tartrate-loaded microneedle patch was performed and independent variables i.e., PVA, HPMC

K4M, and HPMC K15M were optimised. The box-Behnken design was used to analyse the effect of independent variables on the response variables i.e., maximum axial fractured force and cumulative % drug permeated. The quantity of PVA, HPMC K4M, and HPMC K15M were set accordingly to achieve the criteria. The range of quantities was set for PVA (180-220 mg), HPMC K4M (50-60 mg), and HPMC K15M (20-40 mg). A total of 15 batches were prepared based on the experimental design, as mentioned in table 2. The axial fractured force (Y_1) and cumulative % drug permeated at different time intervals (Y_2-Y_8), of prepared microneedle patch were set as a response variable and the effect of the amount of PVA, HPMC K4M, and HPMC K15M were studied as reported in table 4. It was found that the polymer ratio and their total quantities in the microneedle, directly influenced the axial fractured force. PVA is responsible for rigidity and hardness, on increase in the concentration of PVA hardness of the needle increases, so axial fractured force also increases [26]. HPMC K4M and HPMC K15M did not significantly affect needle hardness but contributed to good needle thickness, as shown in 3-D response surface plots fig. 2 and 3. It is important to carefully optimize the PVA content in the formulation to achieve the desired microneedle properties, as too much PVA can lead to brittle needles that break easily, while too little PVA can result in soft needles that may not penetrate the skin effectively. The fractured axial force of optimization batches (BTMN 1-BTMN 15) ranges from 6.25 N to 257.24 N and the design expert software recommended the linear model. It was also found that the concentration of independent variables, mainly HPMC K4M and HPMC K15M affect the cumulative % drug permeated (Y_2-Y_8) at time intervals of 15 min, 30 min, 60 min, 120 min, 240 min, 360 min, 480 min. The 3D response surface plot from fig. 4 to fig. 17, shows that an increase in the concentration of the polymers, mainly HPMC K4M and HPMC K15M, decreases the permeation of the drug. HPMC is a hydrophilic polymer, it can form a gel when it comes into contact with water, which can help to control the release of a drug from the dosage form. The drug permeation rate can be modified by changing the concentration of HPMC in the formulation. HPMC can also be used to modify the release of a drug in a sustained or extended-release formulation [27], in which the drug is released over an extended time. This can be achieved by incorporating HPMC into the formulation so, that it forms a matrix around the drug, which controls the rate at which the drug is released. The cumulative % drug permeated for different level combinations varies from 4.5 % to 38.3 % at 15 min and from 85.2 % to 97.5 % at 480 min as mentioned in table 3.
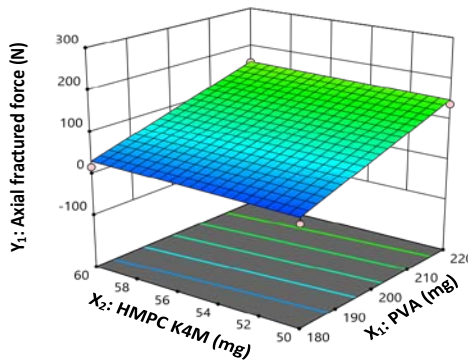

Fig. 2: 3-D response surface plot showing the effect of PVA and HPMC K4M on axial fractured force
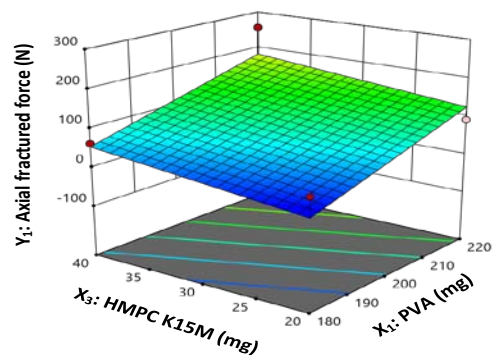

Fig. 3: 3-D response surface plot showing the effect of PVA and HPMC K15M on axial fractured force
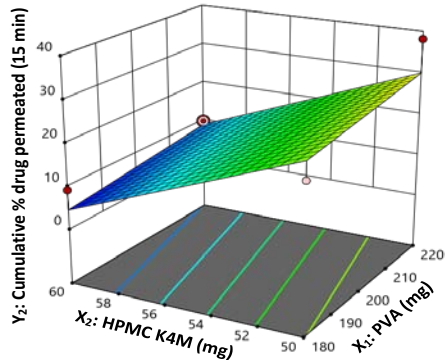

Fig. 4: 3-D response surface plot showing the effect of PVA and HPMC K4M on cumulative % drug permeated (15 min)
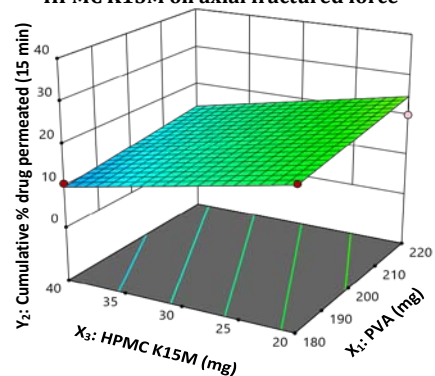

Fig. 5: 3-D response surface plot showing the effect of PVA and HPMC K 15M on cumulative % drug permeated (15 min)
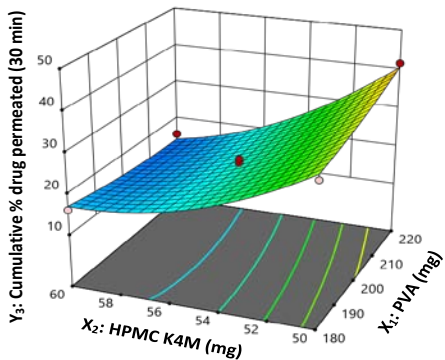

Fig. 6: 3-D response surface plot showing the effect of PVA and HPMC K4M on cumulative % drug permeated (30 min)
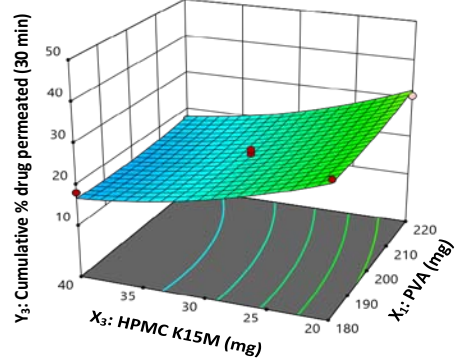

Fig. 7: 3-D response surface plot showing the effect of PVA and HPMC K 15M on cumulative % drug permeated (30 min)
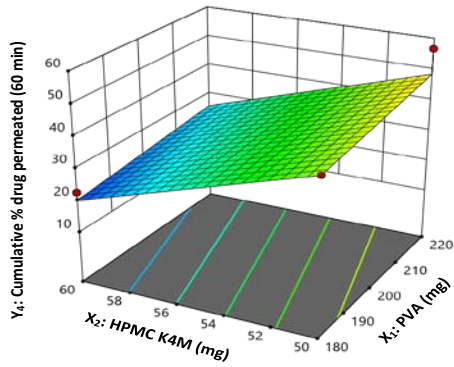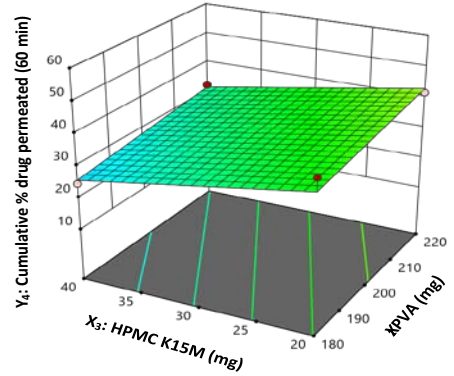
Fig. 8: 3-D response surface plot showing the effect of PVA and HPMC K4M on cumulative % drug permeated (60 min)

Fig. 9: 3-D response surface plot showing the effect of PVA and HPMC K15M on cumulative % drug permeated (60 min)
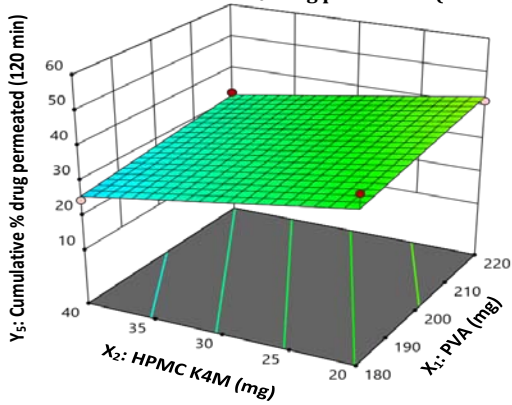

Fig. 10: 3-D response surface plot showing the effect of PVA and HPMC K4M on cumulative % drug permeated (120 min)
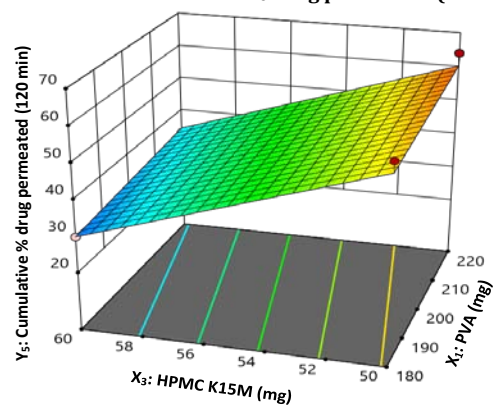

Fig. 11: 3-D response surface plot showing the effect of PVA and HPMC K15M on cumulative % drug permeated (120 min)
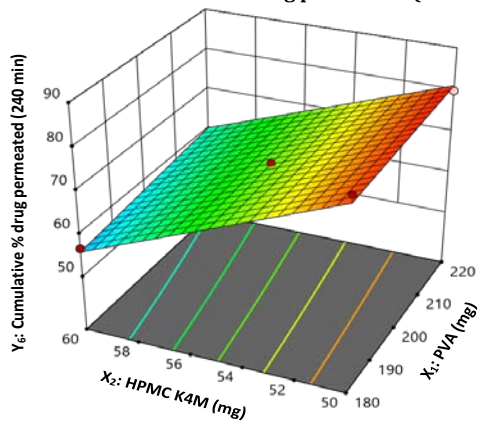

Fig. 12: 3-D response surface plot showing the effect of PVA and HPMC K4M on cumulative % drug permeated (240 min)

Fig. 13: 3-D response surface plot showing the effect of PVA and HPMC K15M on cumulative % drug permeated (240 min)

Fig. 14: 3-D response surface plot showing the effect of PVA and HPMC K4M on cumulative % drug permeated (360 min)
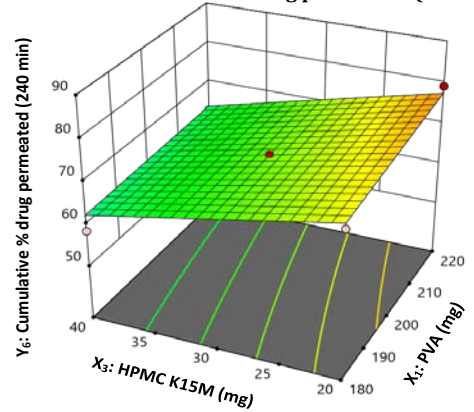

Fig. 15: 3-D response surface plot showing the effect of PVA and HPMC K15M on cumulative % drug permeated (360 min)

Fig. 16: 3-D response surface plot showing the effect of PVA and HPMC K4M on cumulative % drug permeated (480 min)

Fig. 17: 3-D response surface plot showing the effect of PVA and HPMC K15M on cumulative % drug permeated (480 min)
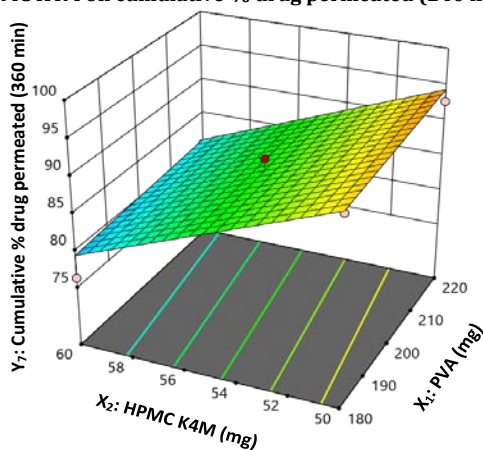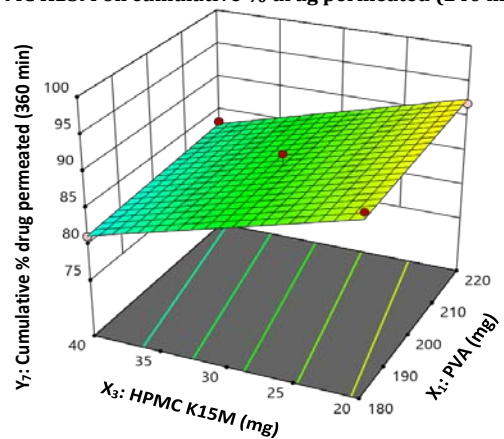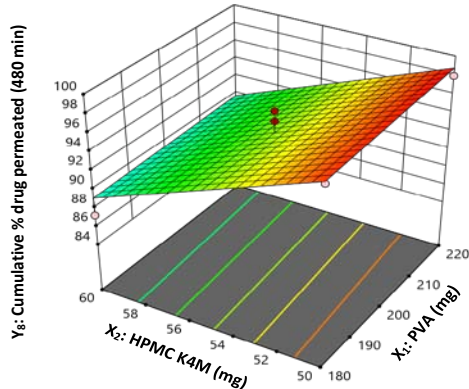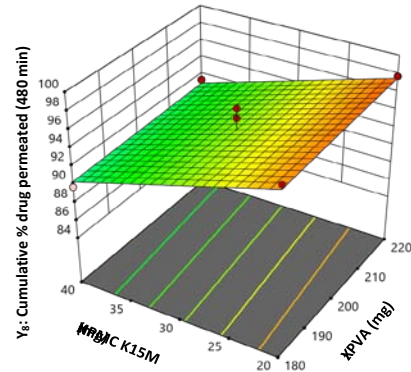
Table 3: Calculated response variables of optimization formulation of butorphanol tartrate loaded microneedle patch

Axial fractured force (N)	Cumulative % drug permeated						
	15 min	30 min	60 min	120 min	240 min	360 min	480 min
6.25±1.26	21.53±0.17	32.26±0.88	42.98±1.42	58.89±1.42	81.87±1.84	92.50±1.11	97.98±0.91
138.47±2.69	38.14±1.37	41.67±1.92	56.63±3.08	64.09±1.78	80.00±6.72	92.74±0.96	97.98±1.67
17.32±0.88	9.29±1.43	16.19±4.58	22.74±3.02	30.12±2.63	56.72±2.13	76.31±3.46	87.26±2.29
157.58±1.73	9.88±0.31	15.60±4.80	23.93±1.27	33.29±3.74	57.98±2.16	80.48±3.96	87.74±2.82
48.70±1.51	20.67±1.62	30.36±2.95	41.43±2.54	51.55±2.97	72.38±0.87	91.89±2.73	97.40±1.77
92.55±2.82	20.24±8.82	30.95±2.82	41.69±5.57	54.17±4.28	79.29±4.16	91.91±2.70	97.74±1.44
62.85±2.19	10.71±2.11	18.21±5.04	24.64±2.25	33.60±5.90	58.48±6.86	81.19±1.99	89.84±3.91
257.34±3.27	11.52±1.53	17.16±1.85	32.26±6.23	40.95±1.38	62.86±7.79	83.21±3.63	91.43±1.17
66.95±2.26	38.33±2.55	46.31±0.20	46.47±0.07	59.13±4.03	81.87±6.20	97.40±0.72	98.81±1.14
69.73±3.11	10.83±1.73	23.45±1.80	33.69±3.58	45.71±3.51	70.24±2.41	89.52±3.71	96.43±1.43
87.1±3.39	21.07±2.32	31.31±2.90	42.62±3.13	55.36±3.68	81.91±2.03	92.26±4.05	97.86±1.65
95.81±1.69	4.52±1.49	10.36±1.05	17.74±3.69	25.83±3.08	50.36±4.10	75.45±4.46	85.24±2.30
85.10±0.95	15.71±2.95	19.05±1.59	28.33±1.50	41.19±1.86	68.33±3.13	85.00±5.62	92.62±1.36
85.21±0.51	14.76±2.98	21.67±3.25	29.17±2.26	41.31±2.43	68.81±5.00	85.60±3.94	95.21±1.83
85.22±0.21	12.62±1.12	22.74±4.17	31.90±1.35	44.05±2.74	69.52±4.01	88.57±3.29	96.26±1.20

Data of the axial fractured force are expressed as mean±SD, n = 3, and cumulative drug permeated data are expressed as mean±SD, n=3.
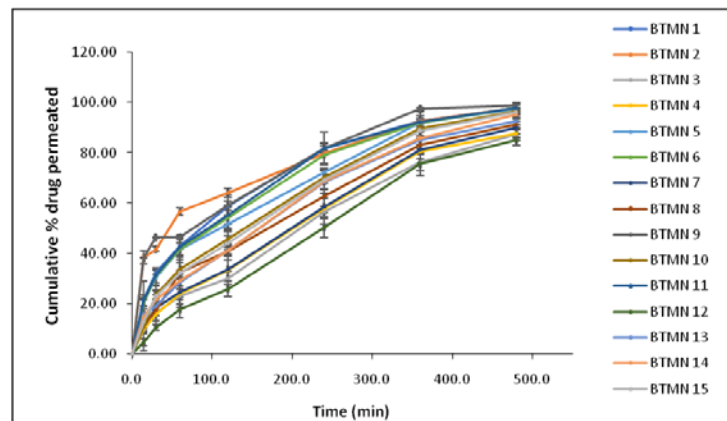

Fig. 18: *In vitro* cumulative % drug permeated of optimization formulation of a butorphanol microneedle patch. All values shown in the graph are measured as mean±SD, n=3 error bar indicates the standard deviation of replicates

Table 4: ANOVA analyse fit summary for butorphanol tartrate loaded microneedle

Responses	Model	Lack of fit p-value	Sequential p-value	Predicted R^2 value	Adjusted R^2 value
Axial fractured force (Y1)	Linear	-	0.0007	0.5141	0.7103
Cumulative % drug permeated at 15 min (Y3)	Linear	0.1055	<0.0001	0.6995	0.8079
Cumulative % drug permeated at 30 min (Y4)	Quadratic	0.5138	0.0252	0.8580	0.9630
Cumulative % drug permeated at 60 min (Y5)	Linear	0.1338	<0.0001	0.7429	0.8207
Cumulative % drug permeated at 120 min (Y6)	Linear	0.1382	<0.0001	0.8360	0.8919
Cumulative % drug permeated at 240 min (Y7)	2FI	0.0409	0.0265	0.8201	0.9396
Cumulative % drug permeated at 360 min (Y8)	Linear	0.4702	<0.0001	0.8152	0.8821
Cumulative % drug permeated at 480 min (Y9)	Linear	0.5098	0.0001	0.6804	0.7929

Table 5: Polynomial equation of response variables

S. No.	Response variable	Polynomial equation
1	Axial fractured force (Y_1)	$90.42+63.85 X_1+5.21 X_2+28.15 X_3$
3	Cumulative % drug permeated (15 min) (Y_2)	$17.32+2.20 X_1-10.57 X_2-5.28$
4	Cumulative % drug permeated (30 min) (Y_3)	$21.15+1.04 X_1-10.74 X_2-6.75 X_3-2.5 X_1X_2-0.4134 X_1 X_3+0.4763 X_2X_3+0.7951$ $X_1^2+4.48 X_2^2+2.22 X_3^2$
5	Cumulative % drug permeated (60 min) (Y_4)	$34.41+2.84 X_1-11.33 X_2-5.75 X_3$
6	Cumulative % drug permeated (120 min) (Y_5)	$45.28+2.29 X_1-12.81 X_2-6.85 X_3$
7	Cumulative % drug permeated (240 min) (Y_6)	$69.37+1.33 X_1-11.3 X_2-6.27 X_3+0.7832 X_1 X_2-0.631 X_1X_3-4.98 X_2X_3$
8	Cumulative % drug permeated (360 min) (Y_7)	$86.94+0.8064 X_1-6.64 X_2-4.83 X_3$
9	Cumulative % drug permeated (480 min) (Y_8)	$93.99+0.3 X_1-4.49 X_2-3.25 X_3$

Where, X_1 = PVA (mg), X_2 = HPMC K4M (mg), X_3 = HPMC K15M (mg)

Prediction of optimized final formulation of butorphanol tartrate loaded microneedle patch

The analysis of the optimization batches and predicted the optimized batch of butorphanol tartrate-loaded microneedle patch was done using Design Expert software. According to the experimental design technique, the formulation with the highest degree of desirability was chosen [28, 29]. The fractured axial force was set at maximum and the cumulative % drug permeated was set at minimum as mentioned in table 1. The design expert software point prediction was used to select an optimized batch of butorphanol tartrate-loaded microneedle based on the desirability close to 1 [30]. The software predicted 54 solutions, and the one with the highest desirability (0.930) was chosen as the optimized formulation batch. The selected formulation had an optimal quantity of independent variables and desired range of response variables, as shown in table 6. The 3D response and contour plot are shown in fig. 19. Graphically representation of experimentally observed *in vitro* cumulative % drug permeated and software predicted *in vitro* cumulative % drug permeated as shown in fig. 20, both had regression (R^2) and correlation coefficients that were extremely near to 1, or 0.994 and 0.997 respectively.

Table 6: Software predicted and experimentally observed variable response data of optimized formulation of butorphanol-loaded microneedle patch

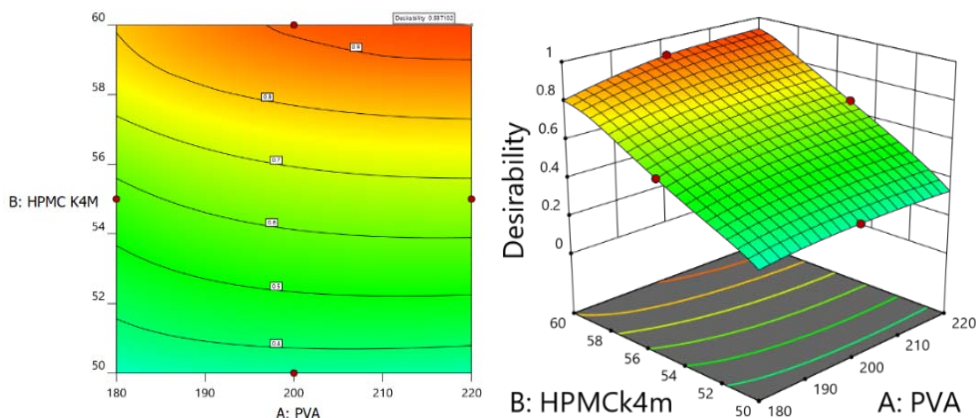| Optimized formulation composition		Response			
Component	Quantity	Evaluation parameter	Software predicted	Experimentally observed value	% Relative error
X_1 = PVA	220.0 mg	Axial fractured force (N)	187.62	189.68±1.66	1.09
X_2 = HPMC K4M	60.0 mg	Cumulative % drug permeated at 15 min	3.67	3.35±0.51	8.63
X_3 = HPMC K15M	40.0 mg	Cumulative % drug permeated at 30 min	9.76	9.54±0.34	8.96
-	-	Cumulative % drug permeated at 60 min	20.17	18.43±0.92	1.41
-	-	Cumulative % drug permeated at 120 min	27.91	29.67±0.97	6.32
-	-	Cumulative % drug permeated at 240 min	48.31	46.34±0.24	4.07
-	-	Cumulative % drug permeated at 360 min	76.27	71.10±0.78	2.82
-	-	Cumulative % drug permeated at 480 min	86.53	89.11±2.17	0.65

Data shown above are measured as mean±SD, n=3.

Fig. 19: 3D response surface graph and contour plot, showing maximum desirability of optimized formulation of butorphanol tartrate loaded microneedle patch

Microscopic evaluation

Laser confocal microscopy

The height, tip diameter, and base diameter of the prepared optimized batch of microneedles (OP-BTMN) were measured using laser confocal microscopy. The microscopic image of laser confocal microscopy of the optimized batch (fig. 21) shows that the average height was 700 μm to 800 μm and the tip diameter was 60 μm to 61 μm; this shows that the microneedle will not reach till pain receptors and thereby making it a painless delivery system for transdermal drug administration [31].
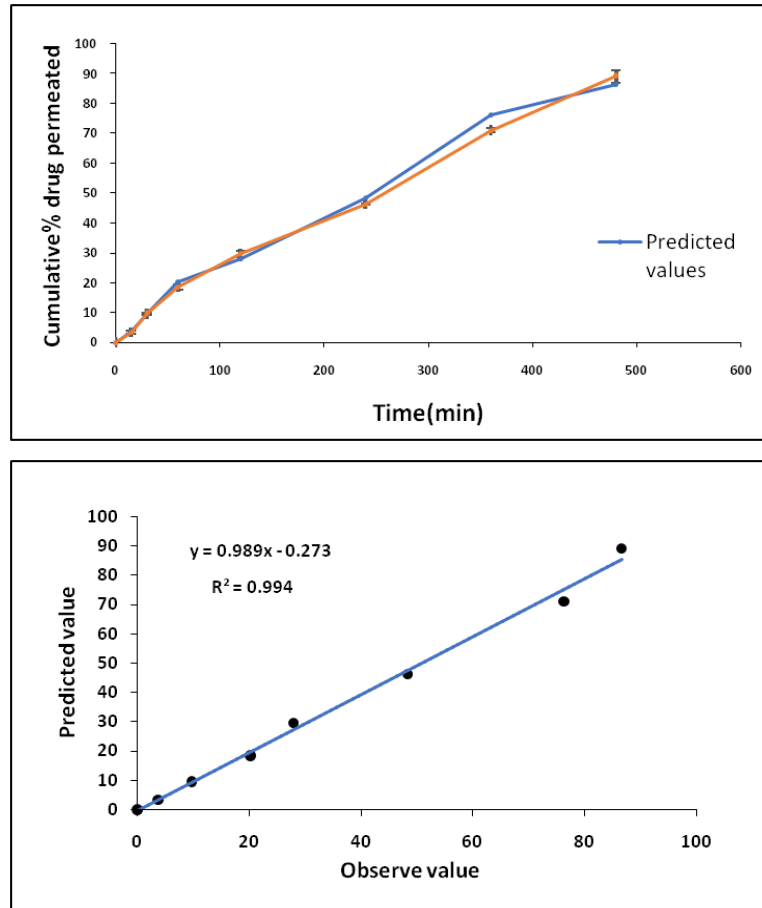
Fig. 20: Software predicted and experimentally observed *in vitro* and regression plot of software predicted versus experimentally observed. Data shown above are measured in mean±SD, n = 3
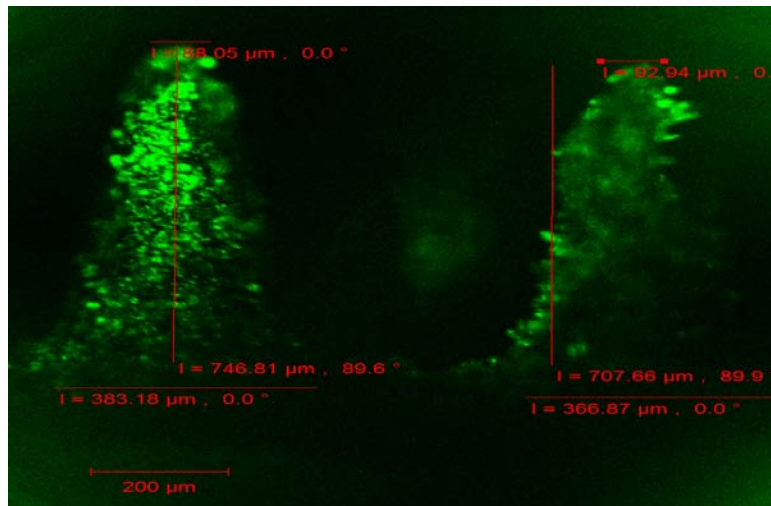

Fig. 21: Laser confocal image of the butorphanol microneedle patch

Scanning electron microscopy

The morphology of microneedles was evaluated using a FESEM (Supra 55 Zeiss) at various magnifications and an accelerating voltage of 2.0 kV. The SEM image (fig. 22) shows that microneedles have a height of less than 1 mm and thickness at the base of around 400 μm and a tip of around 165 μm, which implies that they do not reach the pain receptors and the use of microneedles will result in a painless method for transdermal drug delivery [31].

Axial fractured force

The axial fractured force of the optimized butorphanol tartrate-loaded microneedle patch was calculated using the TA-XT plus texture analyser. The axial fracture force is the least amount of force necessary to be exerted along the axis of a microneedle for the microneedle to break. Higher axial fracture force is required for the microneedles to penetrate the skin [21]. The value of the axial fracture force is found to be 189.68 N [32] and graphically shown in fig. 23.
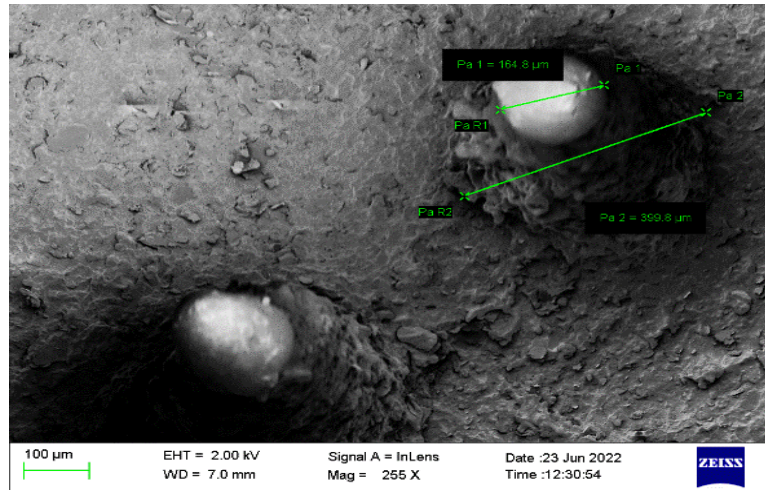
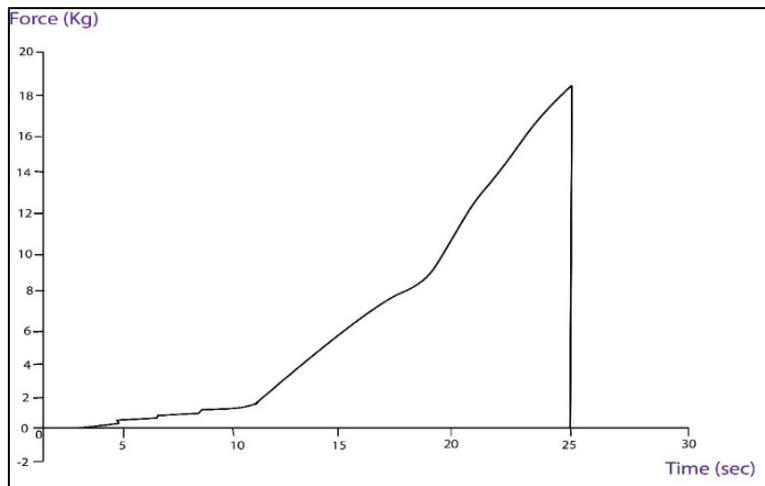**Fig. 22: SEM images of a butorphanol microneedle patch**

Fig. 23: Graph showing the breaking point of the needles of the microneedle array patch

Drug content determination

The drug content of the optimized butorphanol tartrate-loaded microneedle patch was determined in phosphate buffer saline pH 7.4 and was found to be 97.3 %. The drug content of microneedles plays a crucial role in determining the drug delivery efficiency and therapeutic efficacy of the microneedle [33]. If the drug content is too low, it can result in suboptimal drug delivery and a lack of therapeutic effect, while an excessively high drug content can lead to potential toxicity. The result obtained is shown in table 7.

In vitro drug permeation studies for optimized batch

An *In vitro* drug permeation study of the optimized batch (OPBTMN) of the butorphanol tartrate-loaded microneedles was carried out using a Franz-diffusion cell. The graph was plotted between cumulative % drug permeated and time (min) as shown in fig. 24. *In vitro* drug permeation profile of the final optimized batch was examined for different kinetic models and zero-order kinetics showed an R^2 value of 0.9916. This means that the amount of drug permeated at a constant rate irrespective of the concentration of drug present in the system. This type of drug release is typically observed in systems where the drug is released from a solid matrix or a polymer reservoir [34].

Ex-vivo permeation studies

The permeability of butorphanol tartrate-loaded microneedles was assessed for 8 h in the *ex-vivo* permeation studies. The tests were conducted utilising a porcine ear skin on the Franz diffusion cell. The drug permeation from its plain drug solution was found to be 16.59 % at a steady state flow of 0.002 mg/cm²/h, while the drug permeation from the microneedle patch was found to be 38.44 % at a steady state flux of 0.0039 % [32]. It was observed that the permeation enhancement ratio was 1.95. The flux value suggested successful penetration of the stratum corneum by the developed microneedle patches by the formation of microchannels [35]. The graph is shown in fig. 25. The butorphanol tartrate injection and its transdermal patches had been reported in various literature [36-39]. However, the use of dissolving microneedle patches has the advantage of enhancing permeation with painless administration.

Table 7: Drug content determination

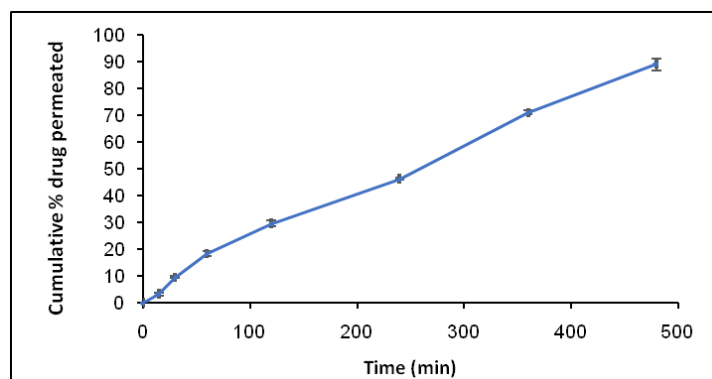| S. No.	Optimized batches	Drug loaded in the microneedle patch	The total drug found in the microneedle patch	Percentage drug content
1	OP-BTMN	3	2.92	97.3%

Fig. 24: Graph between cumulative % drug permeated and time (min) for optimized batch (OPBTMN). Data shown above are measured in mean±SD, n = 3
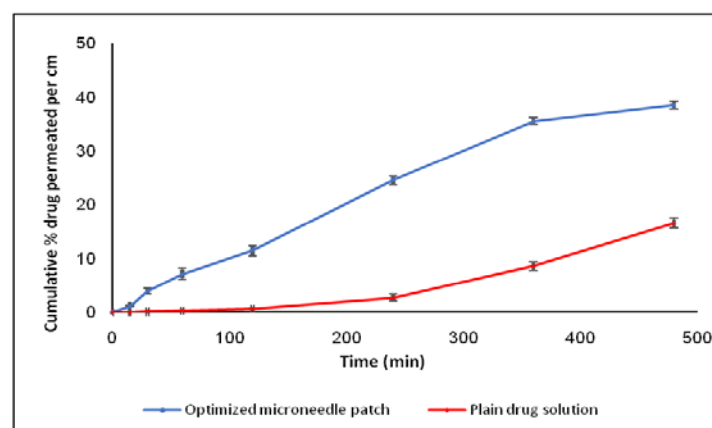

Fig. 25: Graph of cumulative % drug permeated per cm² between MN patch and plain drug solution for *ex-vivo* permeation studies. Data shown above are measured in mean±SD, n = 3

CONCLUSION

In this current research, an effort was made through an experimental design approach to optimize and formulate butorphanol tartrate-loaded microneedle patches. The Box-Behnken design was used to analyse the effect of interactions between responses and factors with selected variables like fractured axial force and *in vitro* drug permeation. The experiment was carried out with three central points with 15 experimental runs in which OP-BTMN is considered the best formulation, which showed the optimum axial fractured force of 189.68±1.66 N and cumulative % drug permeated of 89.12±2.7 for 8 h. Based on the findings, it was concluded that a butorphanol tartrate-loaded microneedle patch can potentially be used to treat postoperative pain with a sustained release effect, the highest loading efficiency and more drug release rate and more permeation efficiency when compared to pure drug solution, which is considered as standard.

AUTHORS CONTRIBUTIONS

All authors have contributed equally.

CONFLICT OF INTERESTS

The authors declare that there is no conflict of interest and other support.

REFERENCES

1. Mazda Y, Jadin S, Kahn JS. Postoperative pain management. Can Journ Gen Int Med 2021;16(SP1):5-17. doi: 10.22374/cjgim.v16iSP1.529.
2. Katz J, Jackson M, Kavanagh BP, Sandler AN. Acute pain after thoracic surgery predicts long-term post-thoracotomy pain. Clin J Pain. 1996 Mar;12(1):50-5. doi: 10.1097/00002508-199603000-00009, PMID 8722735.
3. Sharrock NE, Cazan MG, Hargett MJL, Williams Russo P, Wilson PD. Changes in mortality after total hip and knee arthroplasty over a ten-year period. Anesth Analg. 1995;80(2):242-8. doi: 10.1097/00000539-199502000-00008, PMID 7818108.
4. McQuay H. Opioids in pain management. Lancet. 1999;353(9171):2229-32. doi: 10.1016/S0140-6736(99)03528-X, PMID 10393001.
5. Philip BK, Reese PR, Burch SP. The economic impact of opioids on postoperative pain management. J Clin Anesth. 2002;14(5):354-64. doi: 10.1016/S0952-8180(02)00372-0, PMID 12208440.
6. Dobkin AB, Eamkaow S, Caruso FS. Butorphanol and pentazocine in patients with severe postoperative pain. Clin Pharmacol Ther. 1975;18(5 Pt 1):547-53. doi: 10.1002/cpt1975185part1547, PMID 1102232.
7. Benson HA. Transdermal drug delivery: penetration enhancement techniques. Curr Drug Deliv. 2005;2(1):23-33. doi: 10.2174/1567201052772915, PMID 16305405.
8. Chandrakala V, Chandrakala V, Srinivasan S. An overview: recent development in transdermal drug delivery. Int J Pharm Pharm Sci. 2022;14(10):1-9. doi: 10.22159/ijpps.2022v14i10.45471.
9. Coulman SA, Anstey A, Gateley C, Morrissey A, McLoughlin P, Allender C. Microneedle mediated delivery of nanoparticles into human skin. Int J Pharm. 2009;366(1-2):190-200. doi: 10.1016/j.ijpharm.2008.08.040, PMID 18812218.

10. Milewski M, Brogden NK, Stinchcomb AL. Current aspects of formulation efforts and pore lifetime related to microneedle treatment of skin. Expert Opin Drug Deliv. 2010;7(5):617-29. doi: 10.1517/17425241003663228, PMID 20205604.

11. Prausnitz MR, Langer R. Transdermal drug delivery. Nat Biotechnol. 2008;26(11):1261-8. doi: 10.1038/nbt.1504, PMID 18997767.

12. Donnelly RF, Singh TRR, Tunney MM, Morrow DI, McCarron PA, O'Mahony C. Microneedle arrays allow lower microbial penetration than hypodermic needles *in vitro*. Pharm Res. 2009;26(11):2513-22. doi: 10.1007/s11095-009-9967-2, PMID 19756972.

13. Anjani QK, Permana AD, Carcamo Martinez A, Dominguez Robles J, Tekko IA, Larraneta E. Versatility of hydrogel-forming microneedles in *in vitro* transdermal delivery of tuberculosis drugs. Eur J Pharm Biopharm. 2021;158:294-312. doi: 10.1016/j.ejpb.2020.12.003. PMID 33309844.

14. Carcamo Martinez A, Mallon B, Anjani QK, Dominguez Robles J, Utomo E, Vora LK. Enhancing intradermal delivery of tofacitinib citrate: comparison between powder-loaded hollow microneedle arrays and dissolving microneedle arrays. Int J Pharm. 2021;593:120152. doi: 10.1016/j.ijpharm.2020.120152. PMID 33301867.

15. Quinn HL, Kearney MC, Courtenay AJ, McCrudden MT, Donnelly RF. The role of microneedles for drug and vaccine delivery. Expert Opin Drug Deliv. 2014;11(11):1769-80. doi: 10.1517/17425247.2014.938635, PMID 25020088.

16. Spreen WR, Margolis DA, Pottage Jr JC. Long-acting injectable antiretrovirals for HIV treatment and prevention. Curr Opin HIV AIDS. 2013;8(6):565-71. doi: 10.1097/COH.0000000000000002, PMID 24100877.

17. Manoj VR, Manoj H. Review on transdermal microneedle-based drug delivery. Asian J Pharm Clin Res. 2019;12(1):18-29. doi: 10.22159/ajpcr.2019.v12i1.27434.

18. Vora LK, Donnelly RF, Larraneta E, Gonzalez Vazquez P, Thakur RRS, Vavia PR. Novel bilayer dissolving microneedle arrays with concentrated PLGA nano-microparticles for targeted intradermal delivery: proof of concept. J Control Release. 2017;265:93-101. doi: 10.1016/j.jconrel.2017.10.005. PMID 29037785.

19. Vora LK, Moffatt K, Tekko IA, Paredes AJ, Volpe Zanutto F, Mishra D. Microneedle array systems for long-acting drug delivery. Eur J Pharm Biopharm. 2021;159:44-76. doi: 10.1016/j.ejpb.2020.12.006. PMID 33359666.

20. Wu X, Chen Y, Gui S, Wu X, Chen L, Cao Y. Sinomenine hydrochloride-loaded dissolving microneedles enhanced its absorption in rabbits. Pharm Dev Technol. 2016;21(7):787-93. doi: 10.3109/10837450.2015.1055766, PMID 26122959.

21. Amodwala S, Kumar P, Thakkar HP. Statistically optimized fast dissolving microneedle transdermal patch of meloxicam: A patient-friendly approach to manage arthritis. Eur J Pharm Sci. 2017;104:114-23. doi: 10.1016/j.ejps.2017.04.001. PMID 28385631.

22. Shaji J, Shah A. Optimization of tenoxicam loaded niosomes using quadratic design. Int J Curr Pharm. 2016;8(1):62-7.

23. Kolli CS, Banga AK. Characterization of solid maltose microneedles and their use for transdermal delivery. Pharm Res. 2008;25(1):104-13. doi: 10.1007/s11095-007-9350-0, PMID 17597381.

24. Ferreira PG, Noronha L, Teixeira R, Vieira I, Borba Santos LP, Viçosa A. Investigation of a microemulsion containing clotrimazole and itraconazole for transdermal delivery for the treatment of sporotrichosis. J Pharm Sci. 2020;109(2):1026-34. doi: 10.1016/j.xphs.2019.10.009. PMID 31604084.

25. Klang V, Schwarz JC, Lenobel B, Nadj M, Aubock J, Wolzt M. *In vitro* vs *in vivo* tape stripping: validation of the porcine ear model and penetration assessment of novel sucrose stearate emulsions. Eur J Pharm Biopharm. 2012;80(3):604-14. doi: 10.1016/j.ejpb.2011.11.009. PMID 22123494.

26. Chu LY, Choi SO, Prausnitz MR. Fabrication of dissolving polymer microneedles for controlled drug encapsulation and delivery: bubble and pedestal microneedle designs. J Pharm Sci. 2010;99(10):4228-38. doi: 10.1002/jps.22140, PMID 20737630.

27. Patel DP, Setty CM, Mistry GN, Patel SL, Patel TJ, Mistry PC. Development and evaluation of ethyl cellulose-based transdermal films of furosemide for improved *in vitro* skin permeation. AAPS PharmSciTech. 2009;10(2):437-42. doi: 10.1208/s12249-009-9224-3, PMID 19381831.

28. Ferreira SL, Bruns RE, Ferreira HS, Matos GD, David JM, Brandao GC. Box-Behnken design: an alternative for the optimization of analytical methods. Anal Chim Acta. 2007;597(2):179-86. doi: 10.1016/j.aca.2007.07.011, PMID 17683728.

29. Ortiz MC, Herrero A, Sanllorente S, Reguera C. Methodology of multicriteria optimization in chemical analysis some applications in stripping voltammetry. Talanta. 2005;65(1):246-54. doi: 10.1016/j.talanta.2004.06.031, PMID 18969791.

30. Neufeld L, Bianco Peled H. Designing a biocompatible hydrogel for the delivery of mesalamine. Int J Pharm. 2015;491(1-2):170-9. doi: 10.1016/j.ijpharm.2015.06.026, PMID 26116013.

31. Zhu DD, Chen BZ, He MC, Guo XD. Structural optimization of rapidly separating microneedles for efficient drug delivery. J Ind Eng Chem. 2017;51:178-84. doi: 10.1016/j.jiec.2017.02.030.

32. He J, Zhang Z, Zheng X, Li L, Qi J, Wu W. Design and evaluation of dissolving microneedles for enhanced dermal delivery of propranolol hydrochloride. Pharmaceutics. 2021;13(4). doi: 10.3390/pharmaceutics13040579, PMID 33921712.

33. Rojekar S, Vora LK, Tekko IA, Volpe Zanutto F, McCarthy HO, Vavia PR. Etravirine-loaded dissolving microneedle arrays for long-acting delivery. Eur J Pharm Biopharm. 2021;165:41-51. doi: 10.1016/j.ejpb.2021.04.024, PMID 33971273.

34. Zulcaif N, Zafar N, Mahmood A, Sarfraz RM, Elaissari A. Simvastatin loaded dissolvable microneedle patches with improved pharmacokinetic performance. Micromachines. 2022;13(8):1304. doi: 10.3390/mi13081304, PMID 36014226.

35. Akhtar N. Microneedles: an innovative approach to transdermal delivery-a review. Int J Pharm Pharm Sci. 2014;6(4):18-25.

36. Laniesse D, Smith DA, Knych HK, Mosley C, Guzman DS-M, Beaufrere H. *In vitro* characterization of a formulation of butorphanol tartrate in a poloxamer 407 base intended for use as a parenterally administered slow-release analgesic agent. Am J Vet Res. 2017;78(6):677-87. doi: 10.2460/ajvr.78.6.677, PMID 28541144.

37. Noguchi J, Hatanaka E, Kurita H, Fudoji R, Michinaka Y, Inventors. Google patents, assignee. Patch US. 2019;10(307):381 B2.

38. Sanz MG, Sellon DC, Cary JA, Hines MT, Farnsworth KD. Analgesic effects of butorphanol tartrate and phenylbutazone administered alone and in combination in young horses undergoing routine castration. J Am Vet Med Assoc. 2009;235(10):1194-203. doi: 10.2460/javma.235.10.1194, PMID 19912042.

39. Svozil M, Dolezal P, Hrabalek A, Mericka P. *In vitro* studies on transdermal permeation of butorphanol. Drug Dev Ind Pharm. 2007;33(5):559-67. doi: 10.1080/03639040601128639, PMID 17520448.